ISSN: 2277-9655
Scientific Journal Impact Factor: 3.449
(ISRA), Impact Factor: 2.114

IJESRT

INTERNATIONAL JOURNAL OF ENGINEERING SCIENCES & RESEARCH TECHNOLOGY

EFFECT OF COOLANT JET HOLES ARRANGEMENT ON FILM COOLING PERFORMANCE

Dr. Muwafag Shyaa Alwan*, Dr. Assim H. Yousif, Dr. Amer M. Al-Dabagh
University of Technology, Baghdad, Iraq

ABSTRACT

The film cooling effectiveness and local heat transfer coefficient for coolant jet holes, arrangement, orientation, and inclination angle have been investigated. The tests were carried out using a single test transient IR thermography technique. Evaluation of the cooling performance is obtained by estimated both film cooling effectiveness and heat flux ratios. Two arrangements of coolant jet holes were tested; one is inline holes and the other is staggered holes. Three blowing ratios of (BR= 0.5, 1.0, and 1.5) were used. In order to predict the flow behavior at the holes region, numerical solutions were introduced. It was found that the interaction and diffusion of the coolant air with hot stream present moderate film temperature beyond the downstream row; this flow is mixed with the coming counter vortex pair from downstream row improved the film cooling effectiveness. Experimentally, staggered arrangement gives better coolant performance than that of inline arrangement. The investigation also showed that using the upstream staggered oriented jet over conventional single jet enhanced the average cooling performance by 20.7%, 28.9%, and 37.8% for BR= 0.5, 1.0, and 1.5, respectively.

KEYWORDS: Film cooling, Blowing ratio, Effectiveness, Jet holes arrangement.

INTRODUCTION

Turbine blades require better cooling technique to cope with the increase of the operating temperature with each new engine model. Film cooling is one of the most efficient cooling methods used to protect the gas turbine blades from the hot gases. Jet holes arrangement offers a reliable technique help to improve the coolant effectiveness of the film cooling.

Film cooling primarily depends on the coolant-to-mainstream pressure ratio or can be related to the blowing ratio, temperature ratio (T_c/T_m), the film cooling hole location, configuration, and distribution on a turbine elements film cooling. In atypical gas turbine blade, the range of the blowing ratios is of about 0.5 to 2.0, while the (T_c/T_m) values vary between 0.5 and 0.85 Han and Ekkad (2001)[1].

Injecting behavior of two rows of film cooling holes with opposite lateral orientation angles have been investigated by Ahn et al. (2003)[2],in which the hole rows arrangements were one inline and three staggered. Detailed adiabatic film cooling effectiveness distributions were measured using thermochromic Liquid Crystal to investigate how well the injecting covers the film cooled surface. They found that staggered opposite lateral arrangement shows best cooling performance.

Detailed of heat transfer coefficient and film effectiveness measurements were obtained simultaneously using a single test transient IR thermography technique for a row of cylindrical film cooling hole and shaped holes by Dhungel et al. (2007)[3].They found that the presence of anti-vortex holes mitigates the effect the anti-vortices pairs. Experimental and numerical investigations were done by Lu et al. (2007)[4] to measure and predict the film cooling performance for a row of cylindrical holes. They used adiabatic film effectiveness, and heat transfer coefficients were determined on a flat plate by using a single test transient thermography technique at four blowing ratios of 0.5, 1.0, 1.5 and 2.0.Four test designs, crescent, converging slot, trench and cratered hole exits, were tested. Results showed that both the crescent and slot exits reduce the jet momentum at exit and also provide significantly higher film effectiveness with some increases in heat transfer coefficients.

Numerical prediction of Alwan (2012) [5] shows that the flow field structure of injected holes present

ISSN: 2277-9655
Scientific Journal Impact Factor: 3.449
(ISRA), Impact Factor: 2.114

vortices, such as counter pair kidney vortex and horseshoe vortex have major effects on cooling performance, in which the strength of the kidney vortex decreases and the horseshow vortex is lifting up, leading to an improvement in the coolant performance. Therefore, numerical model is suitable to design holes arrangement futures of film cooling system by introducing oriented holes row over single jet holes row.

NOMENCLATURES

BR blowing ratio
D film hole diameter
h heat transfer coefficient with coolant injection.
ho heat transfer coefficient without coolant injection.
K thermal conductivity of test surface.
q heat flux with coolant injection.
qo heat flux without coolant injection.
T time when the IR image was captured.
T_c coolant air temperature
T_f film temperature
T_i initial temperature
T_m mainstream temperature
T_w prescribed wall temperature
U_c coolant air velocity
U_m mainstream air velocity
η film effectiveness
η_{sa} spanwise average film cooling effectiveness
η_o average film cooling effectiveness
$\emptyset$ overall cooling effectiveness
α thermal diffusivity
γ orientation angle
θ inclination angle
A_o selected area.

EXPERIMENTAL FACILITIES

Low speed open duct test rig was used in the present investigation to supply uniform hot air to the test section. The settling chamber of the test rig contains a series of electrical heaters and row of screen to ensure adequate hot air of uniform temperature throughout the test rig. The hot air was routed through a convergent- divergent contraction having a rectangular cross-section before flowing through the test section. In order to allow the air to reach the desired temperature, the air is initially routed out away from the test section by using a by-bass gate passage. The temperature of the air is continuously monitored at the exit of the gate, and when the desired temperature is reached, the gate is fully opened, and the hot air passes into a test section through a rectangular duct. The operating velocity in the test section is controlled to run from 20 to 40m/s. The test section has 50mm width and 100mm height. The bottom plate of the test section is made of (234x123) mm Plexiglas of 10mm thickness and used as the test model.

A centrifugal air blower was used to supply the coolant air to the plenum. The plenum was located below the test model. The coolant air enters a plenum then ejected through holes into the test section. The coolant air pressure was measured at the inlet of the test section. Digital thermometers were used to measure the mainstream and coolant air temperature. Pre-testing showed that all holes exist constant desired flow rate and temperature.

Two rows of staggered holes with opposite orientation angles are included in the present study. The orientation angles (Ɣ) is defined as the hole orientation toward the cross-flow in the mainstream, and the inclination angle(θ)is defined as the angle between the centerline of the hole and the surface of the test wall, as shown in figure 2. Two models each at different holes arrangement are shown in table (1). Each model supplied with two rows of holes. One of these models is arranged with staggered row holes, the upstream row contains eight holes, while the downstream row is made from seven holes. Another model is inline holes arrangements with eight holes for each row. The holes diameter is 4mm, the longitudinal distance between the upstream and downstream rows (X/D) is 4D, and the span distance between two neighboring holes (S/D) is 3D**.** Data are collected only for three middle holes for each row to reduce the effects of the side wall, as shown in figure (3).

SURFACE TEMPERATURE MEASUREMENT

The surface temperature of test model was measured using an infrared thermographs technique. IR thermograph infrared camera type Fluke Ti32 was used in the present investigation. This camera is able to precisely record the temperature variations. The IR system is greatly affected by both background temperature and local emissivity. The test surface is sprayed with mat black color to increase the emissivity like a perfect black body. The temperature measurement taken is not accurately recorded unless the IR system is calibrated.

The system was calibrated by measuring the temperature of the test surface using thermocouple type K and the reading of IR camera. The test surface is heated by mainstream hot air. The measured

ISSN: 2277-9655
Scientific Journal Impact Factor: 3.449
(ISRA), Impact Factor: 2.114

temperatures obtained by both ways are recorded and stored during the heating process until achieving a steady state condition. Due to the emissivity of the test surface, the temperature obtained by IR camera is different from the temperature obtained by the thermocouple. Therefore, the IR camera reading is adjusted until both temperature readings are matched.

FILM COOLING EFFECTIVENESS AND HEAT TRANSFER COEFFICIENT ESTIMATION

Consider the transient flow over a flat plate. In this case, the test plate is initially at a uniform temperature T_i, and the convective boundary condition is suddenly applied on the plate at time t > 0. Now, the heat is assumed to be conducted only in the x-direction and perform an energy balance on the plate. Therefore the one-dimensional transient conduction equation is

$$\frac{\partial^2 T}{\partial x^2} = \frac{1}{\alpha}\frac{\partial T}{\partial t} \qquad (1)$$

The main approximation often applied to analyze transient conduction shown in Figure 4 is the semi-infinite approximation. The semi-infinite solid assumptions are valid for the present investigation for two reasons. Firstly, the test duration is small, usually less than 60 seconds. Secondly, the hot air flows over the test surface is made from Plexiglas of, low thermal conductivity, low thermal diffusivity, and low lateral conduction. Therefore, the solution of equation (1), as given by Holman et al. (2008)[6] **,** is as follows:

$$\frac{T_w - T_i}{T_m - T_i} = 1 - \exp\left[\frac{h^2 \alpha t}{k^2}\right] erfc\left[\frac{h\sqrt{\alpha t}}{k}\right] \quad (2)$$

Where T_w measured by using IR camera, all the other variables in the equation (2) are either known variables or measured variables except the heat transfer coefficient (h).

In film cooling case, the film should be treated as a mixture of air mainstream and the coolant air, the mainstream temperature (T_m) in equation(2) has to be replaced by the film temperature (T_f).Therefore, equation (2) becomes as:

$$\frac{T_w - T_i}{T_f - T_i} = 1 - exp\left[\frac{h^2 \alpha t}{k^2}\right] erfc\left[\frac{h\sqrt{\alpha t}}{k}\right] \quad (3)$$

A non-dimensional temperature term is known as the film cooling effectiveness (η), and is defined as:

$$\eta = \frac{T_f - T_m}{T_c - T_m} \qquad (4)$$

Equation (3) has two unknowns (h and T_f).To solve this equation, two sets of data points are required to obtain the unknowns like:

$$\frac{T_{w1} - T_i}{T_f - T_i} = 1 - exp\left[\frac{h^2 \alpha t_1}{k^2}\right] erfc\left[\frac{h\sqrt{\alpha t_1}}{k}\right] \quad (5)$$

$$\frac{T_{w2} - T_i}{T_f - T_i} = 1 - exp\left[\frac{h^2 \alpha t_2}{k^2}\right] erfc\left[\frac{h\sqrt{\alpha t_2}}{k}\right] \quad (6)$$

In this case, a transient infrared thermograph technique will be used to obtain both h and η from a single test, as described by Ekkad et al. (2004) [7]. Thus, two images with surface temperature distributions are captured at two different times during the transient test.

A net heat flux ratio is used to measure the combined effect of film effectiveness and heat transfer coefficient Ekkad and Zapata (1997)[8] :

$$\frac{q''}{q_o''} = \frac{h}{h_o}\left(1 - \frac{\eta}{\emptyset}\right) \qquad (7)$$

The value for the overall cooling effectiveness (ø) ranges between 0.5 and 0.7.A typical value is Ø = 0.6 according to Albert et al. (2004)[9], and this in general assumed in the present experimental analysis.The IR images for models surface at each investigated test was captured and stored by a thermal camera.

These images are transferred to PC. Smart View Software program supplied with Camera can be used to limit the selected area to avoid the effect of the test section walls. The IR images converted to corresponding temperature digital values and then saved as data in Excel sheet.

MATLAB Software programs are prepared using a semi-infinite solid assumption to introduce the film cooling effectiveness and heat transfer coefficient contours.

Equations, (4), (5), (6), and (7) may be solved using MATLAB Software, Smart View Software, and Excel Software. The data were collected from the selected area denoted by (A_o);this area included only six staggered jet holes, as shown in Figure (3).

NUMERICAL PROCEDURE

In the present study, air is taken as the working fluid, and the flow characteristics are assumed to be steady flow, Newtonian fluid, incompressible fluid (Mach number=0.11), turbulent flow, and three dimensional. The numerical computation area was matched to the experimental domain instead of computing only two holes with symmetry boundary conditions. FLUENT version (12.1), GAMBIT software and Auto CAD 2011 are be used to create grid for the system geometry and then simulate the film cooling for the

ISSN: 2277-9655
Scientific Journal Impact Factor: 3.449
(ISRA), Impact Factor: 2.114

three geometry models and three blowing ratios. The solution of the Reynolds Averaged Navier-Stokes and energy equations is obtained by using the FLUENT software. Fluent is based on an unstructured solver using a finite volume approach for the solution of the RANS equations. The system geometry shown in figure 4 consists of the box with dimensions (128x12x50) mm for the hot mainstream, box with dimensions (35x12x20) mm for the coolant jet and the different model geometry of two rows of holes, as shown in table 1. The system geometry is drawn by using (Auto CAD 2011 code). The diameter of cooling hole is 4mm.The coolant conditions were maintained the same in all cases, and the mainstream flow rate was altered to change the blowing ratios. The mainstream temperature was set at 322 K, and the coolant temperature was set at 302 K. At the exit plane, the pressure level was specified along with zero streamwise gradients for all other dependent variables.

The current study used the standard $(k-\varepsilon)$model for the simulating the turbulent flows in film cooling. The standard $(k-\varepsilon)$ model is economical with a reasonable accuracy for a wide range of turbulent flows, and it is widely used in heat transfer simulation Versteeg and Malalasekera(1996)[10].There are some general guidelines to create a good mesh. These guidelines are shortly called rules of QRST standing for (Quality, Resolution, Smoothness, and Total cell count) Ozturk(2004) [11].The importance of quality parameter is the face alignment; it is the parameter that calculates skewness of cells. Elements with a high skewness should be avoided. The way of checking whether the solution is grid independent or not is to create a grid with more cells to compare the solutions of the two models. Grid refinement tests for average static temperature on hot surface indicated that a grid size of approximately (2.5 million cell) provides sufficient accuracy and resolution to be adopted as the standard for film cooling system. The nodes near the test plate surface were adjusted; so that average y+ value was about 20 near the test plate surface which is within the range of Jones and Clarke(2005) [12].The most significant factor to be monitored for the present model is the average static temperature on hot surface. When the average static temperature on hot surface value monitor converged, it is unnecessary to go further on with the iterations and wait even if the residuals do not fall below the defined convergence criteria.

RESULTS AND DISCUSSION

Figure (5) shows the film cooling effectiveness variation for different blowing ratios of staggered and inline models. Staggered rows arrangement shows better film cooling effectiveness than the inline model for all blowing ratios under consideration. Film effectiveness values increased as the blowing ratio increased, in which more spreading of coolant air generated in the downstream region as BR increased. Thus, coolant air spreading increased with BRs as (CVP) became strength close to the surface in the parallel plane to the mainstream hot air, as shown in figure (6). The interaction and diffusion of the coolant air with hot stream provided moderate air film temperature flow near the downstream row region, this flow mixed with the coming (CVP) from the downstream row holes leads to high film cooling effectiveness, as shown in figures(7, 8). As indicated by the numerical prediction of Alwan (2012) [5], at BR=0.5 coolant jet flowing toward the surface and hot air departure away from the surface. Among this interested prediction, Ahn et al. (2003) [2] and Yuen and Botas (2005) [13] detected the same trend for staggered and inline rows arrangements both inclined in the same direction.

As a matter of fact, any enhancement of the blade surface protection can be done by keeping the local heat transfer coefficient (h) as low as possible. Figure (9) represents (h) distribution at different BRs. This figure shows that the heat transfer coefficients increases as the blowing ratios increase, in which the turbulence generation increases as BR increases. Staggered arrangement therefore significantly enhances (h) values. These results agree well with the results obtained by Yuen and Botas (2005) [13] for the case of jet holes inclined in the same direction for both hole rows.

Figures (10) represents the spanwise averaged film effectiveness (η_{sa}) distribution. The average values are calculated from the local reading of 46 pixels in spanwise direction in twenty streamlines locations downstream from the hole exist. The streamwise distance between each two successive spanwise locations is equal to (D). For BR=0.5, as shown in figure (10.a), the staggered case gave high values of (η_{sa}) as compared to the inline model. At BR=1.0, the values (η_{sa}) for inline model downstream the hole are higher than those for the staggered model. At (X/D > 2), (η_{sa}) values for the staggered model became higher than the inline model, as shown in Figure (10. b). At BR=1.5, the behavior is similar to that for BR=1.0, but the values of (η_{sa}) for the inline model

ISSN: 2277-9655
Scientific Journal Impact Factor: 3.449
(ISRA), Impact Factor: 2.114

are higher than the staggered model up to (X/D=5), as shown in Figure (10.c).The remarkable differences in these cases under investigation are more likely appear at BR = 0.5.

Comparison also made in Figure (11) with the results of single holes row ($\theta = 30°$) obtained by Lu et al. (2007) [14]. Staggered hole rows are more likely effective (η_{sa}), in which (η_{sa}) increased by 20.7%, 28.9%, and 37.8% from that obtained by Lu et al. (2007) [4**]** for BR= 0.5, 1.0, and 1.5, respectively.

The overall average film cooling effectiveness (η_{av})was calculated from the values of local film cooling effectiveness (η) for the entire pixels values included by the area (A_o). Figure (12) shows the effect of blowing ratio on (η_{av}) for the inline and the staggered models. It was clearly observedthat the values of (η_{av}) for the staggered model are higher than those of inline.

The effect of holes arrangement on the average local heat transfer coefficient ratios (h / h_o), are presented in Figure (13). The values of (h / h_o) for staggered model are higher than those for the inline model for all blowing ratios, (h/ho) increases with increasing BR, in which the injection of the jet produces a high turbulence intensity level inside the mixing region.

In the practical application, turbine designers are concerned with the reduction of heat load to the film protected surface. The heat load can be simulated by combining the film cooling effectiveness (η) and heat transfer coefficient ratio (h/h_o), therefore the ratio (q/q_o) can be introduced to presented the reduction in heat flux at the test surface with the presence of coolant air. If the values of these ratios are less than 1, then the film coolant is beneficial Holman et al. (2008) [6], if the ratio is greater than 1, therefore the film coolant effect has poor performance. Figure (14) shows the effect of BR on (q/q_o). It is clearly observed that the inline and staggered arrangement improve the effects of coolant injected air. Staggered model showed significant reduction in heat flux at all BRs than that for inline model by (28%, 17%, 13%) for the BRs (0.5, 1.0, and 1.5), respectively.

CONCLUSIONS

The present work has reached to the following conclusions:

Staggered arrangement gives better coolant performance and conducts uniform protection than that of inline arrangement.

Near the exit holes area, staggered arrangement shows a uniform heat protection from the hot gas streams.

At low blowing ratio, the film cooling effectiveness is constructed at the holes of exit region, while at high blowing ratio, the coolant jets developing downstream gives better film cooling effectiveness.

The heat flux ratios are found to be less than unity for staggered and inline holes arrangement, (i.e., good enhancement of film cooling effectiveness).

The staggered arrangement enhanced the average cooling performance over the inline arrangements.

REFERENCES

1. Han, J.C. andEkkad, S.V., " Recent Development in Turbine Blade Film Cooling", International Journal of Rotating Machinery, Malaysia, Vol. 7, No. 1, 2001, pp. 21-40.
2. Ahn, J., Jung, I.S., and Lee, J.S., "Film cooling from two rows of holes with opposite behavior and adiabatic film cooling effectiveness", International Journal of Heat and Fluid Flow, Vol. 24, 2003, pp. 91-99.
3. Dhungel, A., Phillips, A., Ekkad, S.V., and Heidmann, J.D., 2007, "Experimental Investigation of a Novel Anti-Vortex Film Cooling Hole Design", ASME IGTI Turbo Expo, Montreal, Paper GT 2007-27419.
4. Lu, Y.,Dhungel, A.,Ekkad, S.V., and Bunker, R.S., 2007, "Effect of Trench Width and Depth on Film Cooling from Cylindrical Holes Embedded in Trenches", ASME Paper GT 2007-27388.
5. Alwan, M.Sh., 2012," Experimental and Numerical Investigation of Film Cooling Thermal Performance for Staggered Rows of Circular Jet", PhD Thesis, Mechanical Engineering Department , University of Technology.
6. Holman, J.P. and Bhattacharyya, S.,2008, "Heat Transfer", Ninth Edition, McGraw-Hill, New Delhi.
7. Ekkad, S.V., Ou, S., and Rivir, R.V., 2004, "A Transient Infrared Thermography Method for Simultaneous Film Cooling Effectiveness and Heat Transfer Coefficient

ISSN: 2277-9655
Scientific Journal Impact Factor: 3.449
(ISRA), Impact Factor: 2.114

Measurements from a Single Test", GT 2004-54236, Proceedings of ASME Turbo Expo, Vienna, Austria.
8. Ekkad, S.V., and Zapata, D., "Heat Transfer Coefficients Over a Flat Surface with Air and CO2 Injection Through Compound Angle Holes Using a Transient Liquid Crystal Image Method", ASME Journal of Turbomachinery, Vol. 119, No. 3, 1997, pp. 580-586.
9. Albert, J.E., Cunha, F. and Bogard, D.G., 2004, "Adiabatic and Overall Effectiveness for a Film Cooling Blade", ASME Paper GT2004-53998.
10. Versteeg, H.K. and Malalasekera, W., 1996, "An Introduction to Computational Fluid Dynamics the Finite Volume Method", Longman Group, London.
11. Ozturk E., 2004, "CFD analysis of heat sinks for CPU cooling with FLUENT", MSc Thesis, Graduate School of Natural and Applied Sciences, Middle East Technical University.
12. Jones, D.A. and Clarke, D.B., 2005, "Simulation of a Wind-body Junction Experiment Using the Fluent Code", DSTD-TR-1731, Australia.
13. Yuen, C. H.N. and Botas, R.F.M., 2005, "Film Cooling Characteristics of Rows of Round Holes at Various Stream Wise Angles in a Cross Flow: Part II Heat Transfer Coefficients", International Journal of Heat and Mass Transfer, London, Vol. 48, PP. 5017-5035.
14. Lu, Y., Dhungel, A., Ekkad, S.V., and Bunker, R.S., 2007, "Film Cooling Measurements for Cratered Cylindrical Inclined Holes", ASME Paper GT 2007-27386.

Table (1) illustrated geometry for the two models

Model Number	Upstream Row		Downstream Row		Shape
	$\boldsymbol{\theta}$	$\boldsymbol{\gamma}$	$\boldsymbol{\theta}$	$\boldsymbol{\gamma}$	
Model1 Stagger	30°	180°	30°	0°	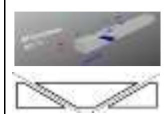
Model2 Inline	30°	180°	30°	0°	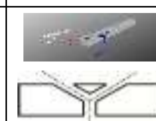

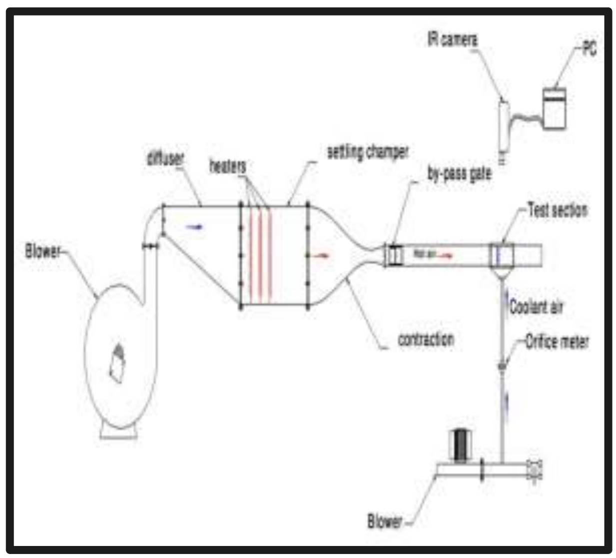

Figure 1 Schematic of the test rig

ISSN: 2277-9655
Scientific Journal Impact Factor: 3.449
(ISRA), Impact Factor: 2.114

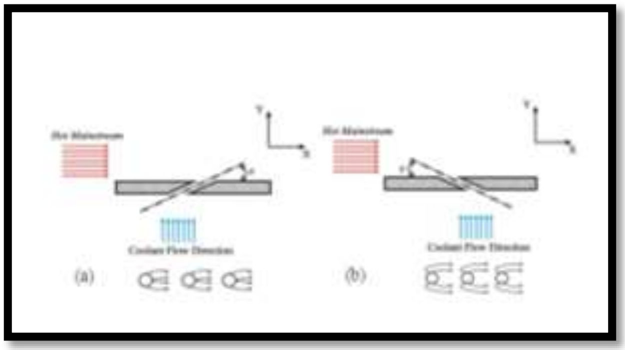

Figure (2) Illustrate diagram of the inclination and orientation angle: (a)$\theta = 30^{\circ}$and $\gamma = o^{\circ}$, (b) $\theta = 30^{\circ}$ and $\gamma = 180^{\circ}$

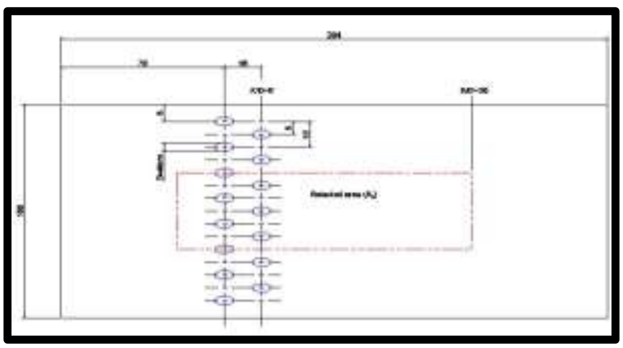

Figure 3 the middle selected area of the test section (A_o)

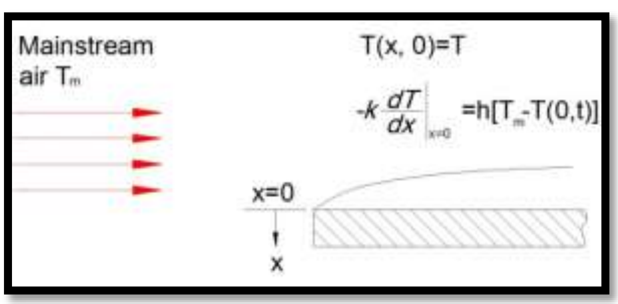

Figure 4 Flow over a flat plate

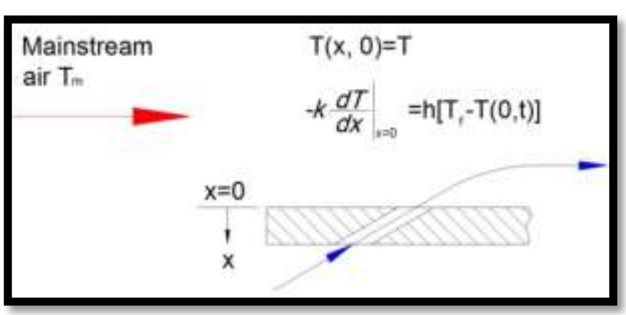

Figure 5 Film cooling over a flat plate

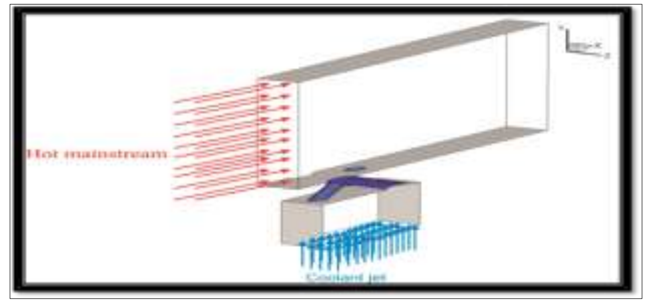

Figure 6 Schematic of geometry shape

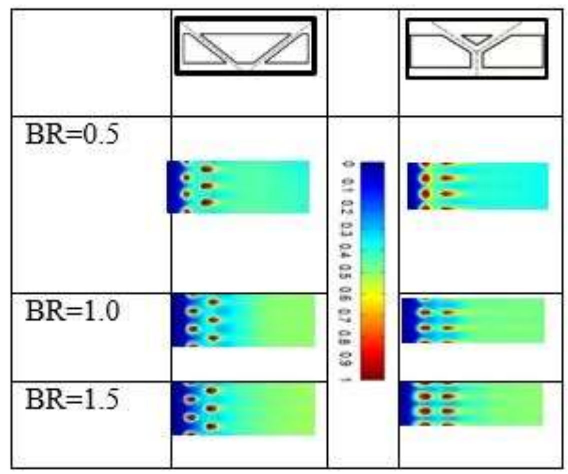

Figure (7) Contours of film cooling effectiveness for hole arrangements (inline and stagger) at different BR. (Exp.)

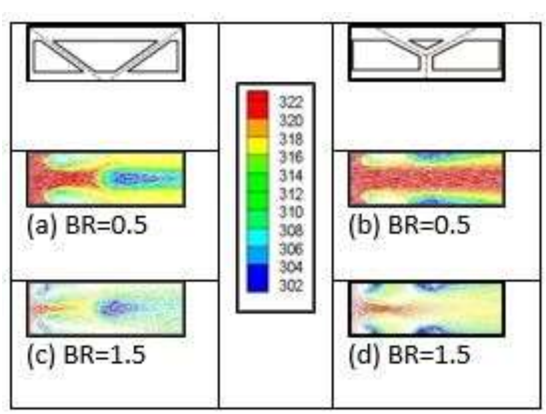

Figure (8) Flow vectors colored by temperature at different planes parallel to test surface for: (a) model 1 BR=0.5, (b) model 2 BR=0.5, (c) model 1 BR=1.5 and (d) model 2 BR=1.5(CFD Fluent 12.1)

ISSN: 2277-9655
Scientific Journal Impact Factor: 3.449
(ISRA), Impact Factor: 2.114

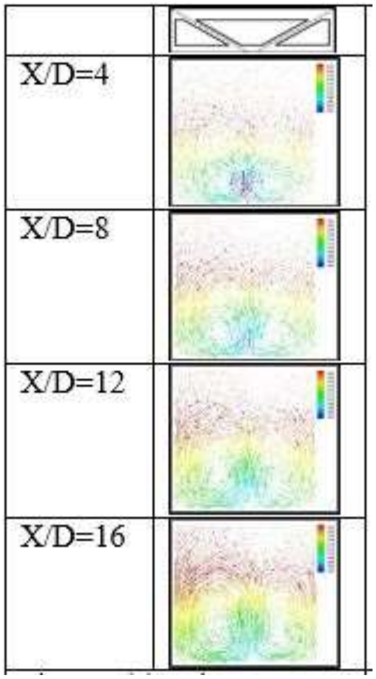

Figure (9) Flow vectors colored by temperature at different span wise planes (X/D=4, 8, 10 and 12) for model (1)at BR=1.0 (CFD Fluent 12.1)

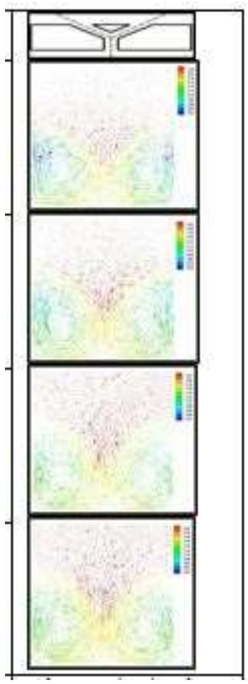

Figure (10) Flow vectors colored by temperature at different span wise planes (X/D=4, 8, 10 and 12) for Model (2)at BR=1.0 (CFD Fluent 12.1)

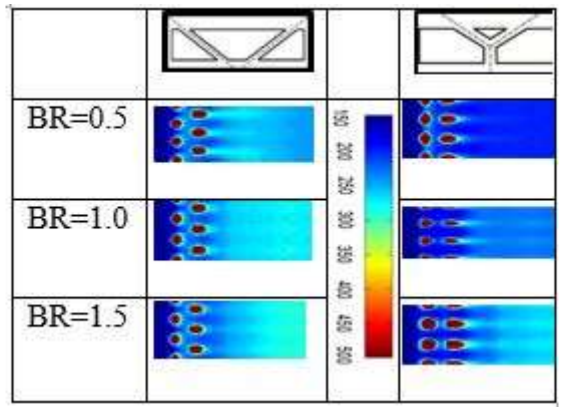

Figure (11) Contours of heat transfer coefficient for hole arrangements (inline and stagger) at different BR. (Exp.)

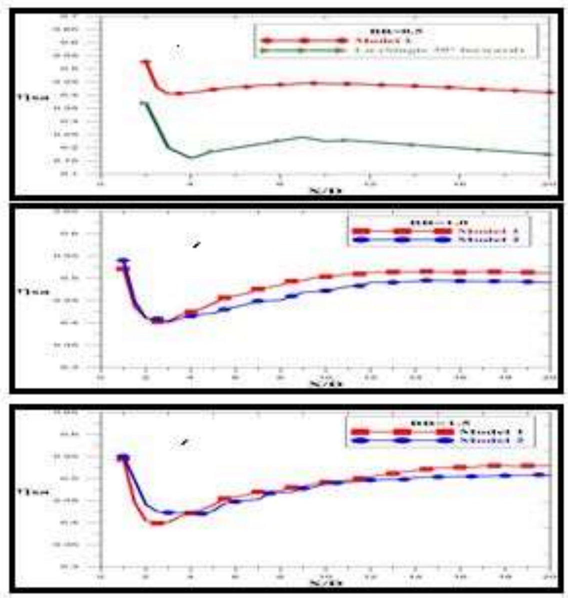

Figure (12) Effect of hole arrangement on span wise averaged film cooling effectiveness at: (a) BR=0.5, (b) BR=1.0, (c) BR=1.5 (Exp.)

ISSN: 2277-9655
Scientific Journal Impact Factor: 3.449
(ISRA), Impact Factor: 2.114

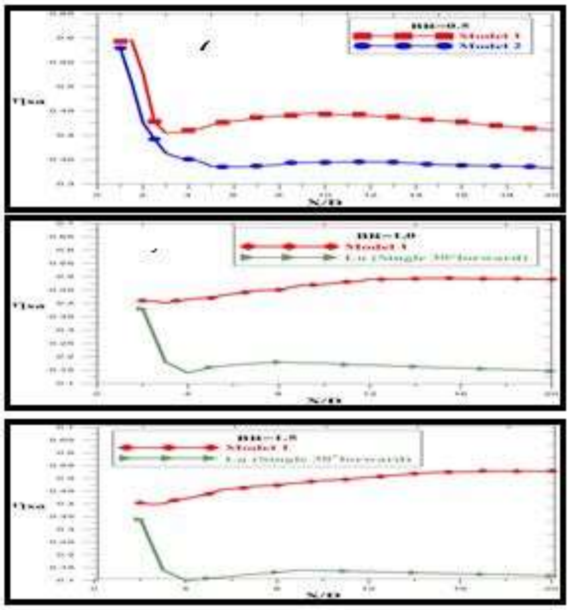

Figure (13) The comparison of the spanwise averaged film cooling effectiveness with Ref. [4] at: (a) BR=0.5, (b) BR=1.0, and (c) BR=1.5.

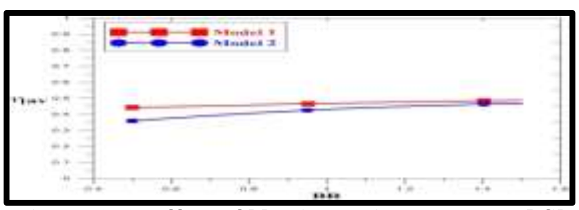

Figure (14) Effect of blowing ratio on averaged film cooling effectiveness (Exp.)

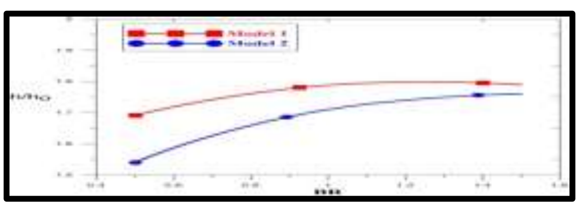

Figure (15) Effect of blowing ratio on averaged heat transfer coefficient. (Exp.)

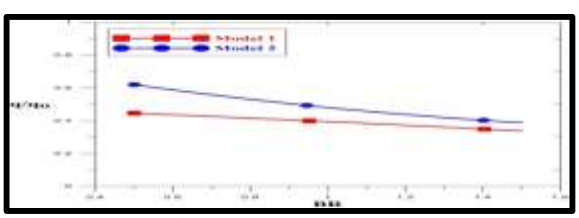

Figure (16) Effect of blowing ratio on overall heat flux ratio.(Exp.)